1. Ahmed Jamal Abdullah Al-Gburi[1], 2. Imran Mohd Ibrahim[1], 3. **Khalid Subhi Ahmad[2],**
4. **Zahriladha Zakaria[1], 5. Mohammed Yousif Zeain[1], 6.M. K. Abdulhameed[3], 7. Tale Saeidi[4]**

[1]Faculty of Electronics and Computer Engineering, Universiti Teknikal Malaysia Melaka (UTeM), Durian Tunggal, Melaka, Malaysia
[2]Department of Electronic Engineering, Northern Technical University, (NTU) 41002 Mosul, Iraq
[3]Ministry of Higher Education and Scientific Research, University of Kerbala, Iraq
[4]Electrical and Electronics Engineering Department, Universiti Teknologi PETRONAS (UTP)
ORCID: 1. 0000-0002-5305-3937; 2.3. 0000-0002-9194-4917; 7. 0000-0002-0995-3364

A miniaturised UWB FSS with Stop-band Characteristics for EM Shielding Applications

Abstract. This paper aims to present a miniaturised and new design of ultra-wideband (UWB) frequency selective surface (FSS) with stopband characteristics for electromagnetic (EM) shielding applications. The modelled FSS used the integration of a two parallel conductive metallic patch with a circular loop structure. The FSS provided a UWB stopband filter response covering a bandwidth of 10.5 GHz, for frequencies from 2.2 GHz to 12.7 GHz. The proposed FSS had a compact physical dimension of 5 mm × 5 mm × 1.6 mm, with a printed array of 19 × 19 FSS unit cells. An equivalent circuit configuration (ECC) was used to verify the FSS unit cell structure's performance. The proposed FSS was identified to contribute towards independent polarisation for obliques incidences transverse electric (TE) and transverse magnetic (TM) polarisations from 0° to 20°. Besides, the performance of the proposed FSS is stable over a wide range of incident angles for TE and TM polarisations.

*Streszczenie. Celem artykułu jest przedstawienie zminiaturyzowanej i nowej konstrukcji ultraszerokopasmowej (UWB) powierzchni selektywnej częstotliwości (FSS) o charakterystyce pasma zaporowego do zastosowań w ekranowaniu elektromagnetycznym (EM). W modelowanym FSS wykorzystano integrację dwóch równoległych przewodzących metalowych łat ze strukturą pętli kołowej. FSS zapewnił odpowiedź filtra pasma zaporowego UWB, obejmującą pasmo 10,5 GHz, dla częstotliwości od 2,2 GHz do 12,7 GHz. Proponowany FSS miał kompaktowy wymiar fizyczny 5 mm × 5 mm × 1,6 mm, z nadrukowaną macierzą 19 × 19 komórek jednostkowych FSS. Do weryfikacji działania struktury komórki elementarnej FSS zastosowano równoważną konfigurację obwodu (ECC). Zaproponowana FSS została zidentyfikowana jako przyczyniająca się do niezależnej polaryzacji dla skośnych padań poprzeczna polaryzacja elektryczna (TE) i poprzeczna magnetyczna (TM) polaryzacja od 0° do 20°. Poza tym wydajność proponowanego FSS jest stabilna w szerokim zakresie kątów padania dla polaryzacji TE i TM. (**Zminiaturyzowany system UWB FSS z charakterystyką pasma zatrzymania do zastosowań w zakresie ekranowania EM**)*

Keywords: Stopband response, ECC, UWB FSS, TE and TM modes, Shielding application
Słowa kluczowe: antena szerokopasmowa, ekranowanie, kompatybilnośc elektromagnetyczna

Introduction

A frequency selective surface (FSS) is any thin, repetitive surface invented to reflect, transmit or absorb electromagnetic (EM) waves based on the incident waves created by FSS. FSSs can be categorised into two types: 1) stopband filter, 2) pass-band filter. These FSSs filters have been widely used in several applications such as radomes EM absorbers, shielding, wearable, meta skin and reflectors [1]–[6]. FSSs with stopband responses can effectively prevent EM interference from passing through it. Moreover, FSS's also have features that change with incidence frequency and polarisation as well. In this sense, FSSs have been extensively used for shielding applications. Few metamaterial structures were designed and introduced in order to create the notch filter rejection [7]–[12]. The Federal Communications Commission (FCC) approved the band's use of 7.5 GHz, from 3.1 to 10.6 GHz, for Ultrawideband (UWB) applications without any license and block interruption with existing spectrums. This is because UWB technology allows the expanse of tiny vibrations in a comprehensive variety of wavelengths [13].

Multi-layer stacks FSS structure with various frequency responses is used to obtain a UWB response [14]–[16]. In [14], A double conductive FSS layer is proposed and provides a bandwidth of 10.8GHz from 5.3-16.1GHz with total dimensions of 12×12×1.6mm. Furthermore, a two sides FSS covering C-band for shielding applications was introduced in [15]. The stated FSS exhibited a bandwidth of 8-12 GHz. Finally, in [16], convoluted FSS was also proposed to obtain a band-stop response, including a frequency range of 3.1–13.3 GHz at 10 dB.

A miniaturised FSS with stopband response is presented in this work. The stated FSS exhibited a fractional bandwidth of 141% in introducing the centre of frequency at 7.45 GHz. Besides, the FSS satisfies polarisation-independent properties due to its proportional geometry. Moreover, the modelled FSS gives a stable response for TM and TE modes.

Proposed FSS Unit Cell Design Strategy
A. FSS Design Process and Characterisation

In this study, the concept of joining two structures was adopted due to the structures' abilities to resonate at a relative frequency to develop an FSS with UWB stopband filter properties. At the same time, the structures' geometries and sizes allowed them to be combined. Hence, finding structures was the first step to design the proposed FSS. In addition, loop models are the best choice as they resonate when their perimeter is approximately a wavelength and their circumferences are good enough to be integrated with other structures. The proposed FSS consisted of a circular loop, which resonates when its circular parties get a part of the wavelength (λ/3), connected to two metallic patches, and their geometries are presented in Fig.1. The FR4 material was used to print the proposed FSS, and the substrate had a dielectric constant of 4.3 with a thickness of 1.6 and 0.02 tangent loss.
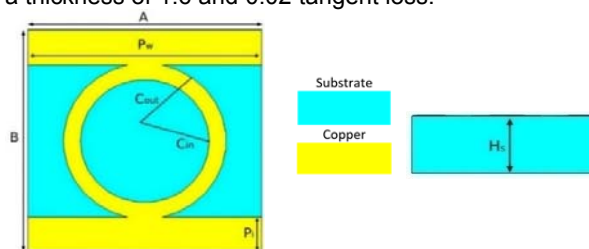

Fig.1. The geometry of the proposed FSS.

A parametric study of the proposed FSS is performed in Fig. 2, and it was mainly developed within three rounds of the design process. The modelled unit cell contained two metallic patches connected with a circular loop. The resonant frequency of the proposed FSS depended on the structure's perimeter, which corresponded to λo at the centre frequency of 7.45 GHz, as displayed in Fig. 2a. A single metallic patch was added and attached to the circular loop geometry. This metallic patch, along with the stationed circular ring, essentially helped deliver stopband operation from 7 GHz up to 14 GHz, as presented in Fig. 2b. The last round was to integrate the circular ring with the two metallic patches. From the simulated results, it was clear that the proposed FSS successfully performed stopband characteristics through UWB frequencies at 6.2 GHz from 2.2 GHz to 12.7 GHz, with a reflection value of 0 dB. The transmission magnitude was less than -10 dB, as presented in Fig. 2c.
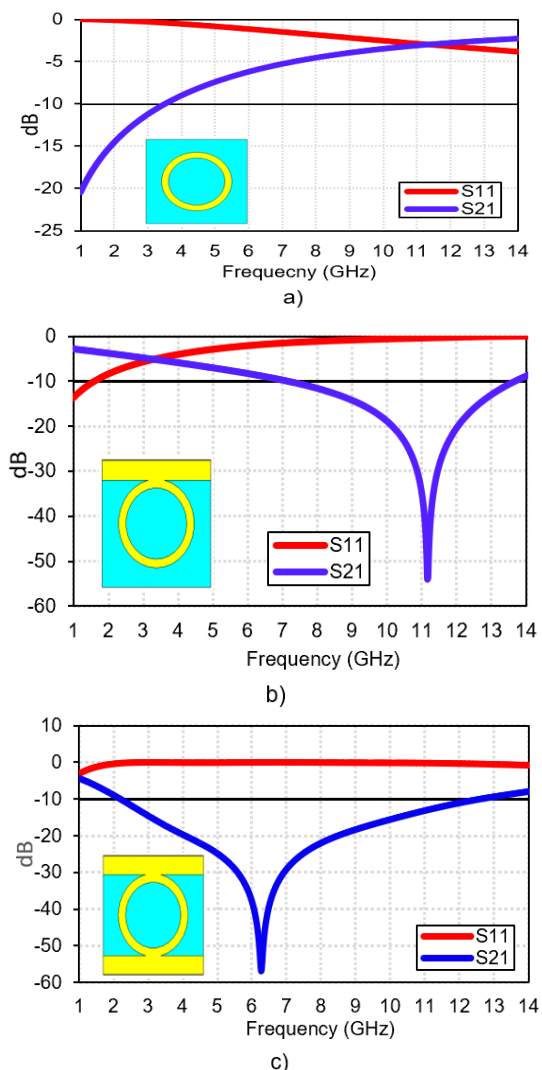

a)

b)

c)

Fig.2. Simulation process of the proposed FSS.

The total physical dimension of the modelled FSS was 5 mm × 5 mm × 1.6 mm (A × B × Hs). The metallic patch width (Pw) was 5 mm, and its length (Pl) was 0.78 mm. An investigation with a comprehensive analysis of the modelled FSS circular loop is presented next.

The circular loop consisted of two essential parameters: "Cin" and "Cout", and these two parameters indicated the edge of the inner and the outer of the circular loop, respectively. Fig. 8 presents the analysis of parameters "Cin" and "Cout" modification effects, which showed that the circular loop corresponded to the modification of its

parameters in a comparable form to the conventional square loop. Additionally, the outer radius was fixed at 1.75 mm.

Fig. 3a shows the effect of different values of "Cin" in which the resonant frequency decreased as the inner circular loop value increased. For example, at 1.7 mm inner circular radius, the stopband response at 4.8 GHz was inadequate compared to other frequencies. As a result, the inner circular radius at 1.7 mm was considered inadequate and thin, and its thickness was made thicker by decreasing the values of the inner ring. Moreover, the stopband response became wider as the inner loop's thickness increased, as can be seen at 1.1 mm of the inner circular radius. Eventually, the optimum inner radius of 1.4 mm was chosen at 6.3 GHz (which is the black colour).

On the other hand, Fig. 3b presents the effect of the outer circular loop for various numbers of "Cout", with the inner radius fixed at 1.7 mm. Developing the outer circular radius led to shifting the resonant frequency to the highest and resulted in wider bandwidth. The optimum outer radius of 1.75 mm was chosen at 6.3 GHz (which is the black colour).

From the aforementioned findings, it can be established that a narrow bandwidth was expected as the inner circular loop became smaller. Likewise, as the outer circular loop became larger, a wider bandwidth with movable resonant frequency was realised. Therefore, it can be concluded that the resonance frequency of the FSS was dependent on the perimeter of its geometry.

The outcomes of the earlier processes assisted in delivering a clear picture of the FSS to act as a stopband as follows:

• Combining the two structures was a great idea that can be used to achieve a stopband response.
• The external edge of the circular ring loop controlled the lower side of its working band
• The internal radius of the circular loop can be used to establish the coveted all higher frequency.
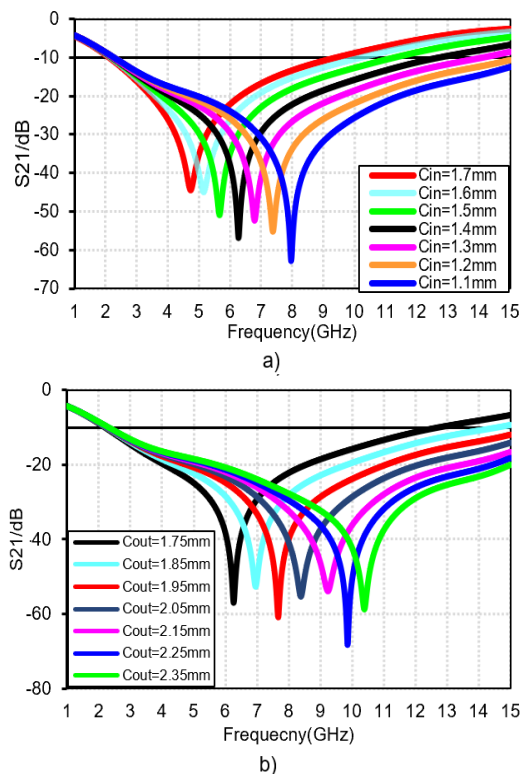

a)

b)

Fig3. Parametric analysis of the proposed circular loop transmission coefficient: a) various values of inner circular loop and b) various values of outer circular loop.

B. ECC and Analysis

The Advanced Design System (ADS) software was used to design the equivalent circuit. The ECC was formed based on the FSS unit cell structure, and afforded inductance (L) and capacitance (C) lumps in the equivalent circuit. In addition, it was modelled based on LC components combined in series (loading 50 Ω), as displayed in Fig. 4. The stopband response was resonating at 6.2 GHz, as presented in Fig. 2c, whereas the load was close to the unit cell's radiation resistance. The input resistance of the equivalent circuit at the stopband was best while its input reactance almost disappeared. As a result, the two metallic patches were produced from the inductance L1, C1, and C2 from the gaps inside and outside the circular ring.
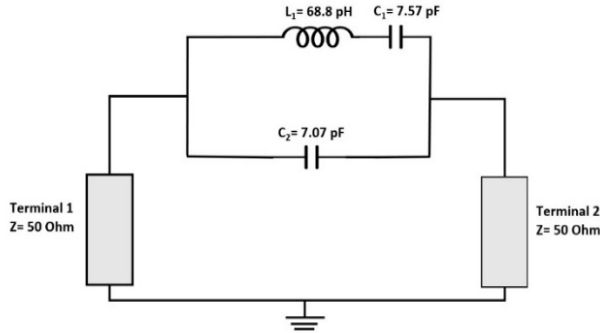

Fig. 4. ECC lump formation.

The vacuum on both ports of the FSS unit structure was represented as a feed line with a neural impedance of $Z_o = 50\ \Omega$. In addition, the neural impedance of the FR4 substrate was represented by $Z_{sub} = \frac{Z_0}{\sqrt{\epsilon_r}} = \frac{50}{\sqrt{4.5}}$.

As aforementioned, the proposed FSS achieved a stopband response at 6.2 GHz, and its lumped derived in equation (2).

$$(1) \qquad Z_{FSS} = \frac{[\omega^2 C_1 - (1-\omega^2 C_1 L_1)(1-\omega^2 C_2)]}{j\omega C_1(1-\omega^2 C_2)}$$

$$(2) \qquad C_2 = \frac{1}{L_1 \omega_{p2}^2}$$

$$(3) \qquad C_1 = \frac{(\omega_{p2}^2 - \omega_{z1}^2)(\omega_{p2}^2 - \omega_{z2}^2)}{-L_2 \omega_{p2}^2 \omega_{z1}^2 \omega_{z2}^2}$$

$$(4) \qquad L_1 = \frac{(-\omega_{z1}^2) - C_1 L_2 \omega_{p2}^2 \omega_{z1}^2}{C_1 \omega_{z1}^2 (\omega_{p2}^2 - \omega_{z1}^2)}$$

The values of the variables ωp1, and ωp2 were the swivel (pole) and zeros pair. Meanwhile, the value of ωp1 was taken to be zero. These variables were realised from equations (9)-(11). The lumped values recorded in Tab.2 were estimated using the equations mentioned earlier.

Table 2: Lumped parameters.

Circuit variables and values			
L_1	C_1	C_2	Z_o
68.8 pH	7.57 pF	7.07 pF	50 Ω

Simulation and Measurement outcomes

The proposed FSS layer is fabricated and printed on an FR4 dielectric substrate of 4.3 of its constant dielectric and 0.02 of tangent loss. The modelled FSS consisting of 19 × 19 unit cells with total dimensions of 100 × 100mm is displayed in Fig. 6.

An attenuator has improved the Impedance match of source and detector. The block diagram used for testing the Transmission coefficient and its schemed in Fig. 5.

Care has been taken to guarantee that the fabricated model replaces the proposed FSS with full consideration of its physical characteristics.
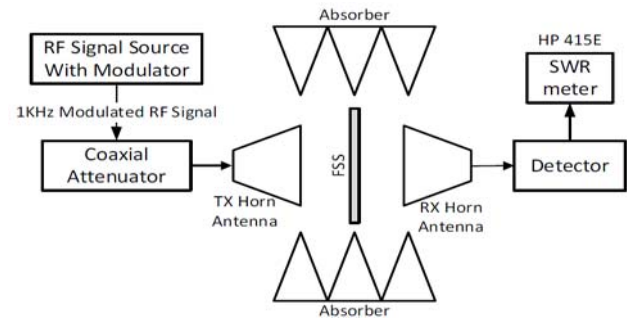

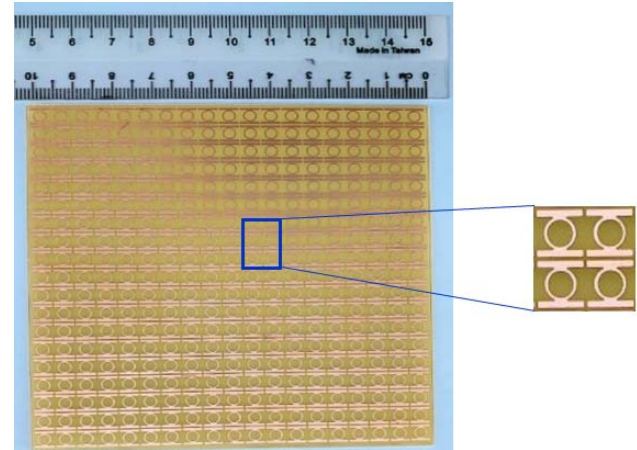Fig. 5. The block of the measurement setup.

Fig.6. Fabricated FSS layer.

The fabricated FSS model placed in an anechoic chamber for measuring the transmission properties.

Two horn antennas are installed fronting the FSS enclosed by the absorbers. The measurement is established by putting horn antennas on both sides of the FSS, configuring them as Sending and Receiving signals towards the antennas, as shown in Fig. 7.
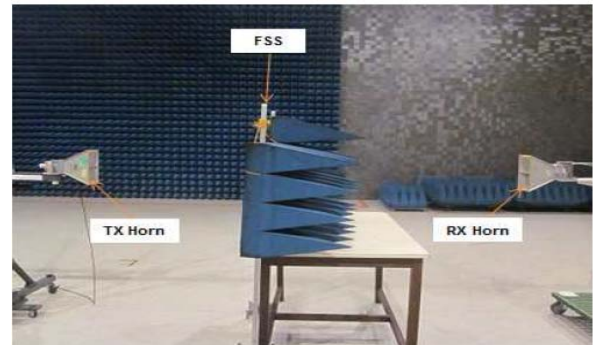

Fig.7. The photo of the measurement setup.

The simulated and measured transmission coefficient (S21) results are portrayed in Fig.8. It's clear that the proposed FSS exhibited a stopband response from 2.2GHz up to 12.7 GHz, with almost -20 dB of return loss performance.

It is evident that the stated FSS gives a comparable transmission behaviour for TE-mode and TM -mode, thus providing polarisation independence.

To examine the angular stability of the modelled FSS, simulation is executed for various aspects of incidence values 0°, 10° and 20°, as depicted in Fig. 8. meanwhile, the stated FSS affords a stable response for both TE and TM polarisation. The notch filter is formed at 6.2 GHz in TE and TM modes, respectively, which is attributed to the FSS geometries.
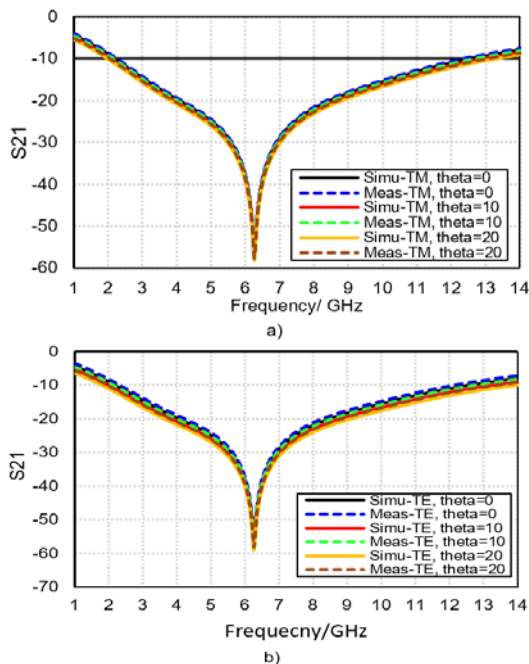
Fig.8. Transmission Coefficient of the finalised FSS for various numbers of the incident angle following a) TM, b) TE.

Conclusion

In this paper, an FSS with electromagnetic shielding property is produced and simulated in a broad spectrum of UWB with a low-cost substrate. The measurement outcomes indicated that the proposed FSS has angular stability in TM and TE polarisations in the range UWB frequencies. Furthermore, simulation outcomes were in high-grade agreement with the measurement outcomes. As a result, the finalised FSS has the potential to use as a reflector to enhance the performance of the planar antennas [17],[18].

Authors: Ahmed Jamal Abdullah Al-Gburi, UTeM university, engahmed_jamall@yahoo.com. Imran Mohd Ibrahim, UTeM university, mranibrahim@utem.edu.my. Khalid Subhi Ahmad, NTU university. jarkovo_1988@yahoo.com. Zahriladha Zakaria, UTeM universty, Zahriladha@utem.edu.my. Mohammed Yousif Zeain, UTeM university, eng.moh1010@gmail.com. Muhannad Kaml Abdulhameed, Ministry of Higher Education and Scientific Research, University of Kerbala, Iraq. Muhannad.k@uokerbala.edu.iq Tale Saeidi, UTP university, tale_g03470@utp.edu.my.

REFERENCES

[1] S. Lamultree, U. Thachantheuk, K. Krasinhom, and C. Phongcharoenpanich, "An Ultra-Wideband Rectangular Monopole with Circular Ring Antenna for Wireless Communication Applications," *Przegląd Elektrotechniczny*, no. 1, pp. 8–11, 2021.

[2] M. Usman, H. Alsaif, H. Alsaif, and S. M. Asif, "Design of Compact Ultra-Wideband Monopole Semi-Circular Patch Antenna for 5G wireless communication networks," *Przegląd Elektrotechniczny*, vol. 2, no. 4, pp. 223–226, 2019.

[3] A. J. A. Al-gburi, I. M. Ibrahim, M. Y. Zeain, and Z. Zakaria, "Compact Size and High Gain of CPW-fed UWB Strawberry Artistic shaped Printed Monopole Antennas using FSS Single Layer Reflector," *IEEE Access*, vol. 8, no. 5, pp. 92697–92707, 2020.

[4] A. Y. I. Ashyap, Z. Z. Abidin, S. H. DAHLAN, and H. A. MAJID, "Highly Efficient Wearable CPW Antenna Enabled by EBG-FSS Structure for Medical Body Area Network Applications," *IEEE Access*, vol. 6, no. 11, pp. 77529–77541, 2018.

[5] A. J. A. Al-gburi *et al.*, "A compact UWB FSS single layer with stopband properties for shielding applications," *Przegląd Elektrotechniczny*, no. 2, pp. 165–168, 2021.

[6] M. Y. Zeain, M. Abu, A. J. A. Al-gburi, Z. Zakaria, R. Syahputri, and A. Toding, "Design of a wideband strip helical antenna for 5G applications," *Bull. Electr. Eng. Informatics*, vol. 9, no. 5, pp. 1958–1963, 2020.

[7] I. M. Ibrahim, A. J. A. Al-gburi, Z. Zakaria, and H. A. Bakar, "Parametric Study of Modified U-shaped Split Ring Resonator Structure Dimension at Ultra-Wide-band Monopole Antenna," *J. Telecommun. Electron. Comput. Eng.*, vol. 10, no. 2–5, pp. 53–57, 2018.

[8] H. H. Keriee, M. K. A. Rahim, N. A. Nayyef, Z. Zakaria, and A. J. A. Al-Gburi, "High gain antenna at 915 MHz for off grid wireless networks," *Bull. Electr. Eng. Informatics*, vol. 9, no. 6, pp. 2449–2454, 2020.

[9] A. J. A. Al-gburi, I. M. Ibrahim, and Z. Zakaria, "Band-notch effect of U-shaped split ring resonator structure at ultra wide-band monopole antenna," *Int. J. Appl. Eng. Res.*, vol. 12, no. 15, pp. 4782–4789, 2017.

[10] R. Adawiyah *et al.*, "Return Loss Improvement of Radial Line Slot Array Antennas on Closed Ring Resonator Structure at 28 GHz," *Prz. Elektrotechniczny*, no. 5, pp. 65–69, 2021.

[11] A. J. A. Al-Gburi, I. Ibrahim, and Z. Zakaria, "Gain Enhancement for Whole Ultra-Wideband Frequencies of a Microstrip Patch Antenna," *J. Comput. Theor. Nanosci.*, vol. 17, no. 2–3, pp. 1469–1473, 2020.

[12] M. Y. Zeain, Z. Zakaria, J. Ahmed, and M. Th, "Design of Helical Antenna for Next Generation Wireless Communication," *Przegląd Elektrotechniczny*, vol. 11, pp. 96–99, 2020.

[13] FCC, "Revision of part 15 of the commission's rules regarding ultra-wideband transmission systems," *First Rep. order*, pp. 2–48, 2002.

[14] M. Mighani and A. Mallahzadeh, "New UWB Shielding with Frequency Selective Surfaces," *J. Commun. Eng.*, vol. 6, no. 1, pp. 71–80, 2017.

[15] D. Kanchana, S. Radha, B. S. Sreeja, and E. Manikandan, "Convoluted FSS Structure For Shielding Application In X-Band Frequency Response Convoluted FSS Structure For Shielding Application In X-Band Frequency," *IETE J. Res.*, vol. 2, no. 1, pp. 1–7, 2019.

[16] S. S. Sampath and R. Sivasamy, "A Single-Layer UWB Frequency-Selective Surface With Band-Stop Response," *IEEE Trans. Electromagn. Compat.*, vol. 62, no. 1, pp. 276–279, 2019.

[17] A. J. A. Al-gburi *et al.*, "High Gain of UWB CPW-fed Mercedes-Shaped Printed Monopole Antennas for UWB Applications," *Prz. Elektrotechniczny*, no. 5, pp. 70–73, 2021.

[18] A. J. A. Al-gburi, I. M. Ibrahim, and Z. Zakaria, "Gain Enhancement for Whole Ultra-Wideband Frequencies of a Microstrip Patch Antenna," *J. Comput. Theor. Nanosci.*, vol. 17, pp. 1469–1473, 2020.